Inositol 1, 4, 5-trisphosphate receptor is required for spindle assembly in *Xenopus* oocytes

Ruizhen Li[a], Yanping Ren[a,b], Guolong Mo[a,c], Zackary Swider[d,e], Katsuhiko Mikoshiba[f,g], William M. Bement[d,e], and X. Johné Liu[a,c,h,*]

[a]Ottawa Hospital Research Institute, The Ottawa Hospital—General Campus, Ottawa, ON K1H 8L6, Canada; [b]Department of Histology and Embryology, Zunyi Medical University, Zunyi, Guizhou 563003, China; [c]Department of Biochemistry, Microbiology and Immunology and [h]Department of Obstetrics and Gynaecology, University of Ottawa, Ottawa, ON K1H 8M5, Canada; [d]Graduate Program in Cellular and Molecular Biology and [e]Center for Quantitative Cell Imaging, University of Wisconsin—Madison, Madison, WI 53706; [f]SIAIS ShanghaiTech University, Middle Huaxia Road, Shanghai 201210, China; [g]Faculty of Science, Toho University Miyama, Funabashi, Chiba, 247-8510 Japan

ABSTRACT **The extent to which calcium signaling participates in specific events of animal cell meiosis or mitosis is a subject of enduring controversy. We have previously demonstrated that buffering intracellular calcium with 1,2-bis(2-aminophenoxy)ethane-N,N,N′,N′-tetraacetic acid (BAPTA, a fast calcium chelator), but not ethylenebis(oxyethylenenitrilo)tetraacetic acid (EGTA, a slow calcium chelator), rapidly depolymerizes spindle microtubules in *Xenopus* oocytes, suggesting that spindle assembly and/or stability requires calcium nanodomains—calcium transients at extremely restricted spatial–temporal scales. In this study, we have investigated the function of inositol-1,4,5-trisphosphate receptor (IP_3R), an endoplasmic reticulum (ER) calcium channel, in spindle assembly using Trim21-mediated depletion of IP_3R. Oocytes depleted of IP_3R underwent germinal vesicle breakdown but failed to emit the first polar body and failed to assemble proper meiotic spindles. Further, we developed a cell-free spindle assembly assay in which cytoplasm was aspirated from single oocytes. Spindles assembled in this cell-free system were encased in ER membranes, with IP_3R enriched at the poles, while disruption of either ER organization or calcium signaling resulted in rapid spindle disassembly. As in intact oocytes, formation of spindles in cell-free oocyte extracts also required IP_3R. We conclude that intracellular calcium signaling involving IP_3R-mediated calcium release is required for meiotic spindle assembly in *Xenopus* oocytes.**

Monitoring Editor
Sarah Wignall
Northwestern University

Received: Jun 22, 2022
Revised: Sep 13, 2022
Accepted: Sep 16, 2022

INTRODUCTION

Formation of the meiotic spindle in animal oocytes is a fundamental early step in development: deficits in spindle assembly or function result in abnormal chromosome partitioning, failure of meiotic polar body emission (asymmetric cytokinesis), or both. These in turn cause aneuploidy in the oocyte, which, depending on its severity, can result in birth defects, catastrophic failure of embryogenesis and resultant infertility (Plachot *et al.*, 1987). However, in contrast to mitotic spindle assembly, which has been the subject of intense interest for more than a century, meiotic spindle assembly in animal oocytes remains relatively poorly understood. That meiotic spindle assembly differs significantly from mitotic spindle assembly is indicated by its positioning—one pole closely abuts the cortex of the oocyte; by its organization—it lacks centrosomes; and by its function—meiotic spindles must execute two closely spaced anaphases in the absence of an intervening S-phase (Liu, 2012).

The special features of the meiotic spindle imply the existence of special regulatory mechanisms. One such mechanism is the calcium "nanodomain." Calcium nanodomains are highly focal regions of elevated intracellular free calcium, previously proposed to control

This article was published online ahead of print in MBoC in Press (http://www.molbiolcell.org/cgi/doi/10.1091/mbc.E22-06-0218) on September 21, 2022.
Conflicts of interest: The authors declare that they have no conflict of interest.
*Address correspondence to: Johné Liu (jliu@ohri.ca).

Abbreviations used: BAPTA, 1,2-bis(2-aminophenoxy)ethane-*N*,*N*,*N*′,*N*′-tetraacetic acid; BSA, bovine serum albumin; CSF, cytostatic factor; DB-BAPTA, dibromo-BAPTA; EGTA, ethylenebis(oxyethylenenitrilo)tetraacetic acid; ER, endoplasmic reticulum; GST, glutathione S-transferase; GVBD, germinal vesicle breakdown; hCG, human chorionic gonadotropin; i. p., intra-peritoneum; IP3R, inositol-1,4,5-trisphosphate receptor; MI, metaphase I; MII, metaphase II; NPB, nuclear preparation buffer; OCM, oocyte culture medium, used for long-term oocyte incubation/maintenance; OR2, oocyte incubation medium, used for short-term oocyte incubation; PMSG, pregnant mare serum gonadotropin.

processes such as exocytosis in neurons (Wang and Augustine, 2014). Such domains are characteristically sensitive to fast calcium chelators, such as BAPTA, but insensitive to slower calcium chelators, such as EGTA (Adler *et al.*, 1991). Consistent with a role for calcium nanodomains in meiotic spindle assembly, we recently found that buffering intracellular calcium via either microinjection of BAPTA or UV-mediated release of BAPTA causes rapid spindle disruption in *Xenopus* oocytes, whereas microinjection of EGTA has no effects (Li *et al.*, 2016).

Calcium nanodomains require that a source of calcium be closely opposed to the nanodomain target. We therefore reasoned that if *Xenopus* meiotic spindles are indeed regulated by calcium nanodomains, the spindles must have a proximal calcium source, and that disruption of this source should impair spindle assembly. We focused on the ER and on inositol 1,4,5-trisphosphate receptor (IP_3R), which regulates IP_3-induced release of calcium from the ER lumen (Taylor and Tovey, 2010). We chose IP_3R as it is the only known ER calcium channel expressed in *Xenopus* oocytes (Kume *et al.*, 1993) and because ER is commonly associated with spindles (Parry *et al.*, 2006; Lu *et al.*, 2009) including in mouse oocytes (FitzHarris *et al.*, 2007; Mann *et al.*, 2010). We employed the "TrimAway" antibody-mediated protein degradation strategy (Clift *et al.*, 2017, 2018) to deplete oocyte IP_3R and assess the consequences of this depletion for meiosis and meiotic spindle assembly. We also developed a novel cell-free spindle assembly assay involving individual oocytes to further characterize the consequences of IP_3R depletion and other manipulations on meiotic assembly. Using these approaches, we show that IP_3R and calcium signaling are required for meiotic spindle assembly and maintenance.

RESULTS AND DISCUSSION

Depletion of IP_3R in *Xenopus* oocytes using TrimAway

TrimAway refers to the combined use of antibodies for a particular target protein and Trim21, an antibody-binding ubiquitin ligase that specifically ubiquitinates antibody-bound target proteins, resulting in their proteolysis (Clift *et al.*, 2017, 2018). While TrimAway has been employed previously to target specific proteins in *Xenopus* embryos (Weir *et al.*, 2021), its use in *Xenopus* oocytes has not been described previously. We therefore first tested the efficacy of this approach by microinjecting mRNA encoding mCherry fused to Trim21 (mCh-Trim), anti-IP_3R antibodies, or both into immature oocytes and then processing samples for immunoblotting (see *Materials and Methods*). Relative to uninjected controls, the combination of mCh-Trim and anti-IP_3R antibodies resulted in apparently complete depletion of IP_3R (Figure 1A). Consistent with previous results (Clift *et al.*, 2017), neither the antibody alone nor mCh-Trim alone resulted in IP_3R depletion (Figure 1A). To assess the specificity of the antibodies, we compared the results obtained with TrimAway of IP_3R (i.e., GFP-Trim with anti-IP_3R antibodies) and those obtained with TrimAway of glutathione S-transferase or GST (i.e., GFP-Trim with anti-GST antibodies; Bayaa *et al.*, 2000). In contrast to IP_3R TrimAway, GST TrimAway failed to deplete IP_3R (Figure 1B). Finally, we addressed the speed with which TrimAway depleted IP_3R by first expressing GFP-Trim overnight, microinjecting anti-IP_3R antibodies the following day, and then processing samples for immunoblotting 30 min, 1, 2, or 4 h after antibody injection. The results indicated that depletion commences within 30 min of antibody injection and is complete within 4 h (Supplementary Figure S1). We conclude that TrimAway is a powerful approach for acute depletion of proteins in *Xenopus* oocytes and, more specifically, that it permits efficient removal of IP_3R.

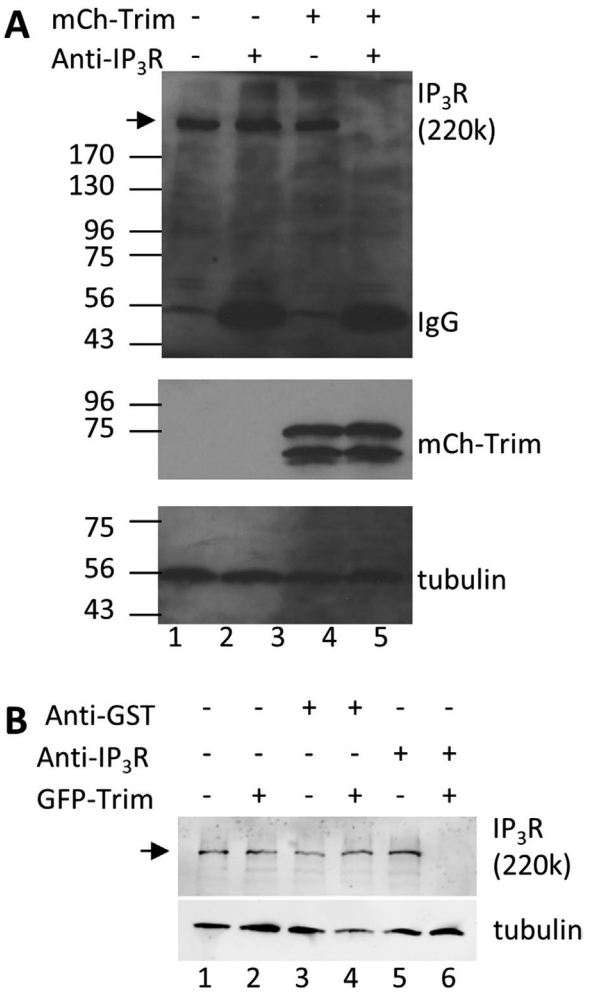

FIGURE 1: TrimAway IP_3R in *Xenopus* oocytes. (A) Control oocytes and oocytes injected with mCherry-Trim21 mRNA were incubated for 24 h followed by injection with anti-IP_3R antibodies, as indicated. Oocytes were lysed 4 h after antibody injection for immunoblotting, first using anti-IP_3R antibodies followed by and anti-β-tubulin antibodies. Molecular weight markers are shown. Arrow depicts IP_3R. Representative of three independent experiments. (B) Control oocytes and oocytes injected with eGFP-Trim21 mRNA were incubated for 24 h followed by injection with anti-IP_3R antibodies or anti-GST antibodies, as indicated. Four hours following antibody injection, oocytes were lysed for immunoblotting using anti-IP_3R antibodies or anti-tubulin antibodies. Arrow depicts IP_3R. Representative of three independent experiments.

Depletion of IP_3R disrupts polar body emission and meiotic spindle assembly

Meiotic maturation in *Xenopus* oocytes is triggered by progesterone treatment and entails germinal vesicle breakdown (GVBD), followed by formation of the first meiotic spindle, first meiotic anaphase, emission of the first polar body, and then formation of the second meiotic spindle, after which the oocytes remain arrested at the second metaphase until fertilization. To assess the potential involvement of IP_3R in meiosis, oocytes were subjected to IP_3R TrimAway, treated with progesterone, and then allowed to progress to the point of metaphase II arrest. While IP_3R depletion had no effect on GVBD (indicating that it is not required for normal activation of cyclin-dependent kinase 1), it significantly impaired completion of oocyte maturation. That is, while 94% of uninjected oocytes

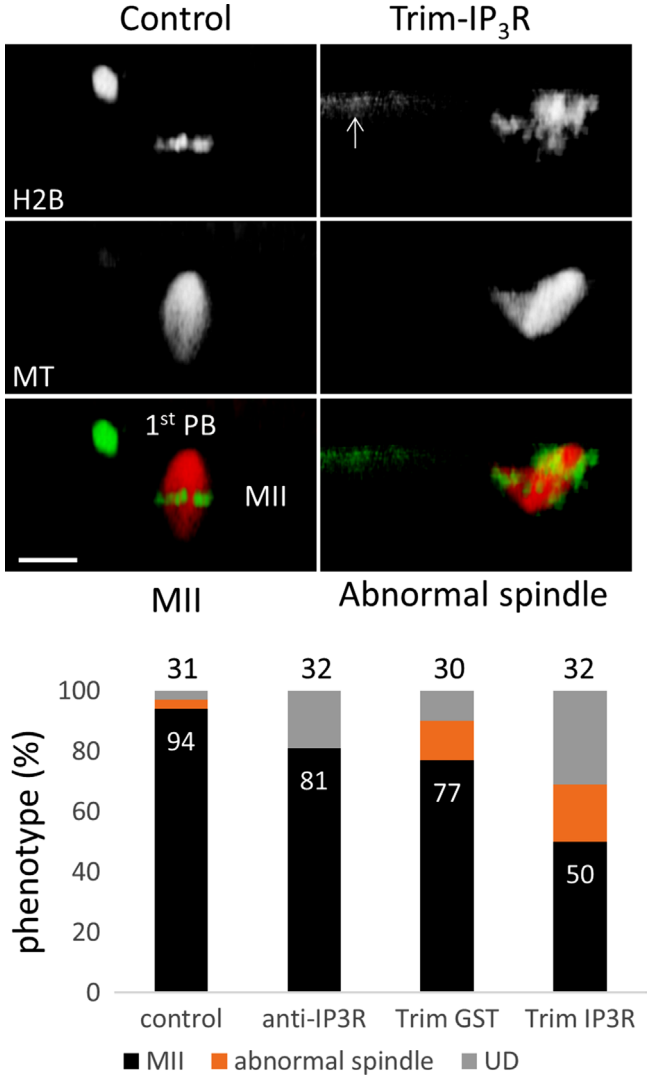

FIGURE 2: IP_3R depletion inhibited first polar body formation. Oocytes injected with mRNAs coding for RFP-tubulin (red) and eGFP-H2B (green) were further injected with GFP-Trim21 mRNA as indicated (Trim). Twenty-four (24) hours after Trim21 mRNA injection, oocytes were injected with anti-IP_3R antibodies or anti-GTS antibodies as indicated. Four hours after antibody injection, all oocytes were incubated with progesterone overnight before being examined by confocal microscopy. Oocytes were recorded as metaphase II (MII, with a first polar body and a bipolar metaphase II spindle; scale bar = 20 μm), abnormal spindle (no polar body; arrow depicts oocyte cortex), or undetectable (UD) (no chromosomes seen within the depth of the confocal system, not shown). The graph summaries five independent experiments depicting the proportions of oocytes exhibiting the three phenotypes. Percentage of MII oocytes in each group is indicated within the bar, with total oocyte number indicated above.

successfully arrested at metaphase II, as judged by the presence of a first polar body and a metaphase II spindle with one pole anchored to the cortex (Figure 2, control), only 50% of oocytes subjected to IP_3R TrimAway successfully reached the same stage (Figure 2, Trim IP_3R). This increase in failed metaphase II in IP_3R TrimAway samples from that in uninjected controls was significant (χ^2, p = 0.0002), as well as that in oocytes injected with anti-IP_3R antibodies (χ^2, p = 0.0169) alone, or oocytes subjected to GST TrimAway (χ^2, p = 0.0378). Furthermore, among the IP_3R TrimAway oocytes that failed metaphase II, some exhibited grossly abnormal spindles but no polar body (Figure 2, abnormal spindle); others (undetectable or UD) exhibited no polar body or chromosomes within the imaging depth of our confocal system (~50 μm from the oocyte surface; not shown), although these oocytes had undergone GVBD, as indicated by the presence of depigmented "maturation spot" in the animal pole. Thus, IP_3R is required for normal meiosis and, in particular, polar body emission.

A novel oocyte-based in vitro spindle assembly assay reveals a dependence on IP_3R in bipolar spindle assembly

The above results demonstrated that IP_3R is required for normal polar body emission. While the simplest explanation for failed polar body emission is that it arises from improper spindle assembly, it could also arise from improper spindle positioning. Further complications arise from the challenge inherent in imaging meiotic spindle dynamics in the large (~1.2 mm–diameter), yolky *Xenopus* oocyte such that only spindles present at or near the oocyte cortex can be detected by epifluorescence or conventional confocal microscopy. We therefore sought a means to assay meiotic spindle assembly under conditions where the impact of IP_3R depletion on meiotic spindle assembly could be more easily and more directly assessed. Cytoplasmic extracts made from *Xenopus* eggs are well established to support spindle assembly in vitro when combined with demembranated *Xenopus* sperm (Maresca and Heald, 2006), however, such extracts are generated by crushing thousands of ovulated eggs in high-speed centrifugation, meaning that manipulations that entail prior microinjections are impossible.

To overcome this limitation, we devised a microaspiration approach that permitted spindle assembly in extracts obtained from individual *Xenopus* oocytes (see *Materials and Methods* and Supplemental Figure S2). Oocytes expressing markers for DNA (eGFP-histone H2B; used to label sperm chromosomes as they exchange protamine for histone during spindle assembly) and microtubules (RFP-tubulin) were incubated in OCM (oocyte culture medium, *Materials and Methods*) with progesterone. Following GVBD, an oocyte was transferred directly to an optical dish under oil and impaled with a micropipette and cytoplasm was aspirated and then transferred onto demembranated *Xenopus* sperm (Lohka and Masui, 1983) under oil. As with bulk extracts made from ovulated eggs (Maresca and Heald, 2006), the aspirated cytoplasm supported spindle assembly: within a few minutes of mixing the cytoplasm with demembranated sperms, a microtubule aster formed (Figure 3A, 00:00) and quickly transformed into a monopolar (00:09) and then bipolar (00:15 and 00.21) spindle; accompanying the microtubule rearrangements, the sperm nucleus transformed into individual chromosomes that aligned in the middle of the bipolar spindle. The spindles apparently executed anaphase, pulling all chromosomes to one pole (00:24; 9/9 or 100%) before microtubules disappeared (00:33), followed immediately by chromosome disappearance (sank into the droplet, beyond the imaging depth of our confocal systems, not shown). About 1 h later, metaphase II spindles could be seen that remained stable, often for hours. The lack of chromosome segregation during anaphase is perhaps anticipated, since sperm chromosomes exist as single, unpaired sisters and therefore have only one kinetochore each. This contrasts with the chromosome separation and bipolar movement shown in previous experiments using cytostatic factor (CSF)-arrested *Xenopus* egg extracts following calcium elevation, which triggers S phase before spindle assembly and anaphase (Desai *et al.*, 1998).

Spindle assembly was also carried out in extracts derived from metaphase II–arrested oocytes, equivalent to the classical CSF extracts (Maresca and Heald, 2006). To prevent inadvertent calcium-mediated oocyte activation, metaphase II (MII) oocytes were rinsed

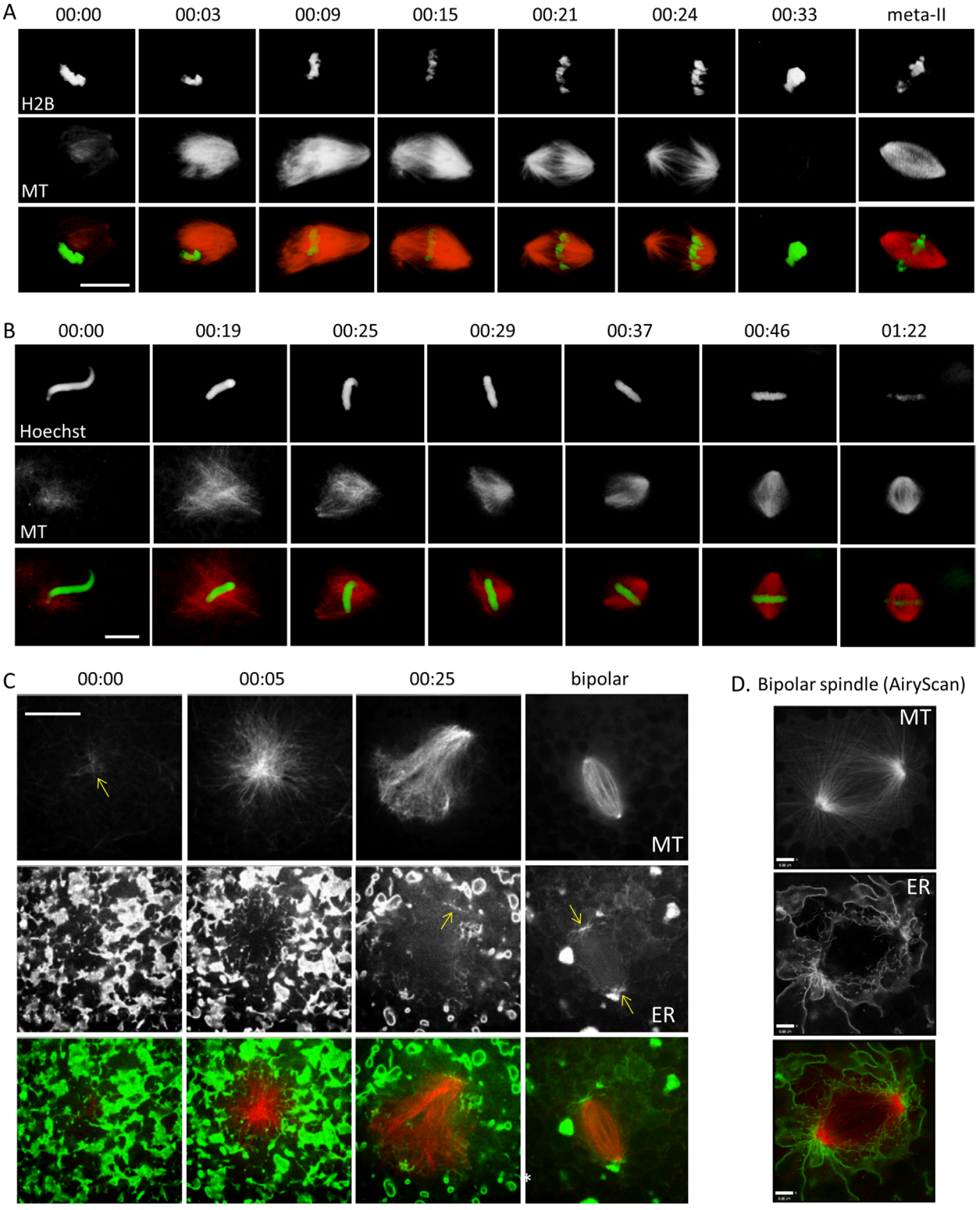
A
00:00
00:03
00:09
00:15
00:21
00:24
00:33
meta-II
H2B
MT
B
00:00
00:19
00:25
00:29
00:37
00:46
01:22
Hoechst
MT
C
00:00
00:05
00:25
bipolar
MT
ER
D. Bipolar spindle (AiryScan)
MT
ER
E
IP3R/MT/DNA

in calcium-free OR2 plus 5 mM EGTA (see *Materials and Methods* for details) before being placed under oil. Spindle assembly in MII extracts proceeds to bipolar spindles similarly to that in MI extracts but remains in the bipolar state, often for hours (Figure 3B). Similar MII extracts were used in all experiments described below.

If ER and IP_3R are important for generating spindle-associated calcium nanodomains in oocyte extract–derived spindles, they should localize near spindles assembled from oocyte extracts. To monitor the distribution of ER, we employed sfGFP-ER-3, an ER marker consisting of the ER-targeting sequence of calreticulin (including the KDEL ER retention peptide) and superfolder (sf)GFP (see *Materials and Methods* for details). sfGFP-ER was expressed in oocytes via DNA injection, together with RFP-tubulin. Within a few minutes after mixing MII cytoplasmic droplets with sperm, an aster could be seen amongst the evenly distributed ER membranes (Figure 3C, 00:00, arrow). The aster rapidly increased in microtubule bulk (Figure 3C, 00:05) and transformed to a monopolar spindle (Figure 3C, 00:25) and then a bipolar spindle (Figure 3C, bipolar). Accompanying this microtubule reorganization, the ER membranes underwent dramatic transformation around the forming spindle. Specifically, the evenly distributed ER membranes near the aster (Figure 3C, 00:00), best described as complex three-dimensional interconnected ER tubules (Terasaki *et al.*, 2001), was gradually replaced by thinner ER tubules permeating the enlarging aster (Figure 3C, 00:05), and then concentrating at the monopole (Figure 3C, 00:25, arrow) and both poles of the bipolar spindle (Figure 3C, bipolar, arrows). The intimate relationship between the spindle poles and these ER tubules can be further appreciated in high-resolution images of bipolar spindles (Figure 3D, AiryScan). To monitor the distribution of IP_3R, GFP-IP_3R1 (Bannai *et al.*, 2004) was expressed in oocytes together with mCh-tubulin. Like ER, GFP-IP_3R1 was first seen associated with ER membranes evenly distributed in the cytoplasm (Figure 3E, left) but became highly concentrated near the poles of the bipolar spindles (Figure 3E, right).

To determine if the ER is required for spindle maintenance in oocyte extracts, samples were treated with Triton X-100 to permeabilize the ER. Triton treatment of bipolar spindles resulted in both the loss of the spindle-associated ER and the disassembly of the spindle itself (Figure 4A) suggesting that the ER is needed for spindle maintenance. To determine if the ER is required for spindle assembly, triton was added to the extract prior to spindle assembly. This treatment prevented bipolar spindle assembly, although it did not prevent microtubule polymerization per se (Figure 4B), consistent with an earlier study (Groen *et al.*, 2011).

To determine if IP_3R is required for spindle assembly, we compared extracts derived from control oocytes, oocytes microinjected with anti-IP_3R antibodies alone, oocytes subject to GST TrimAway or oocytes subject to IP_3R TrimAway with respect to their capacity to support formation of bipolar spindles. Control oocyte extracts supported robust bipolar spindle assembly (Figure 4C), while extracts from oocytes microinjected anti-IP_3R antibodies alone or oocytes subject to GST TrimAway exhibited a slight but significant inhibition of bipolar spindle assembly (Figure 4C). In contrast, extracts subject to IP_3R TrimAway displayed a severe deficit in spindle assembly, with more than 75% failing to support formation of bipolar spindles (Figure 4C). This failure rate was significantly different from those for any of the other three groups (χ^2; $p < 0.0001$, $p = 0.0001$, and $p < 0.0001$ when compared with control, anti-IP_3R, and Trim GST respectively). Instead, sperm chromosomes were found disorganized, clustered with microtubule bundles or scattered with few microtubules (Figure 4C, Trim-IP_3R, left and right, respectively). In addition, we observed microtubule asters (see Figure 4B, right) or nuclei (indicative of exit of metaphase II and entering interphase), although these phenotypes (other) appeared in all three treated groups (Figure 4C). These results, taken with those from intact oocytes, indicate that IP_3R is required for proper meiotic spindle assembly. The reason for the apparently greater effect of IP_3R deficiency on spindle assembly in vitro (Figure 4C) compared with that in intact oocytes (Figure 2) is not clear. One possibility might be that cytoplasmic aspiration induces further Trim21-mediated degradation of IP_3R.

As an independent test of the role of IP_3R, bipolar spindles assembled in oocyte extracts were subject to treatment with heparin, an IP_3R antagonist (Groigno and Whitaker, 1998) or, as a control, calcium free OR2 (the vehicle for heparin). Infusion of heparin into extract containing spindles resulted in disassembly of spindle microtubules (Figure 4D, middle and bottom rows) while infusion of the same volume of calcium-free OR2 had no effect (Figure 4D, top row). The reason for the variable length of time, from 7.5 to 20 min (Figure 4D, graph), to completely disrupt spindles in heparin-infused

FIGURE 3: A novel cell-free spindle assembly system. (A) MI extracts: oocytes expressing RFP-tubulin (red) and eGFP-H2B (green) are stimulated to undergo meiosis. Cytoplasm is aspirated from an MI oocyte (1hour after GVBD) and mixed with demembranated sperm nuclei. An aster was seen about 5 min after mixing (00:00; hh:mm), which rapidly enlarged (00:03) and became a monopolar (00:09) and then bipolar (00:15 and 00:21) spindle. Anaphase was observed where all chromosomes moved to the same pole (00:24) before microtubules disappeared (00:33) (9/9 or 100%). Metaphase II spindles appeared 1 h later (5/9 or 56%) and remained stable. Scale bar = 20 µm. (B) MII extracts: time series (hh:mm) of bipolar spindle formation from a single sperm in cytoplasm aspirated from a metaphase II arrested oocyte expressing RFP-tubulin (red). Hoechst dye (1 µg/ml) was added to sperm droplet to visualize DNA (green). The bipolar spindle is stable, usually for hours. Time 0 represents 5 min after mixing the cytoplasm with sperm. Scale bar = 20 µm. (C) Representative stages of extract spindle assembly in oocytes expressing sfGFP-ER3 (DNA injection) and RFP-tubulin. An aster formed in the microtubule-and ER tubules-rich oocyte extracts (00:00), which rapidly enlarged and was permeated by thinner ER tubules (00:09). In monopolar (00:25) and bipolar spindles, the thinner ER tubules were found concentrated at the poles (arrows). The bright ER blob (*) represented circular ER tubule stack. Scale bar = 20 µm. Shown are representative of >10 independent experiments. (D) High-resolution (AiryScan) single-plane confocal images through the center of a bipolar spindle assembled in cell-free cytoplasmic extract expressing sfGFP-ER3 and RFP-tubulin. Scale bar = 5 µm. Shown are representative of >10 independent experiments. (E) Enrichment of IP_3R at spindle poles: Oocytes were injected with GFP-IP_3R1 plasmid DNA and RFP-tubulin mRNA. Cytoplasmic extracts were aspirated from metaphase II-arrested oocytes and mixed with sperm droplets containing Hoechst dye (1 µg/ml). (Left) A microtubule aster was seen associated with a sperm 5 min after cytoplasm and sperm were mixed. (Right) A bipolar spindle depicting close association of spindle poles and IP_3R-positive ER elements. Scale bar = 5 µm. Shown are representative images obtained in two independent experiments.

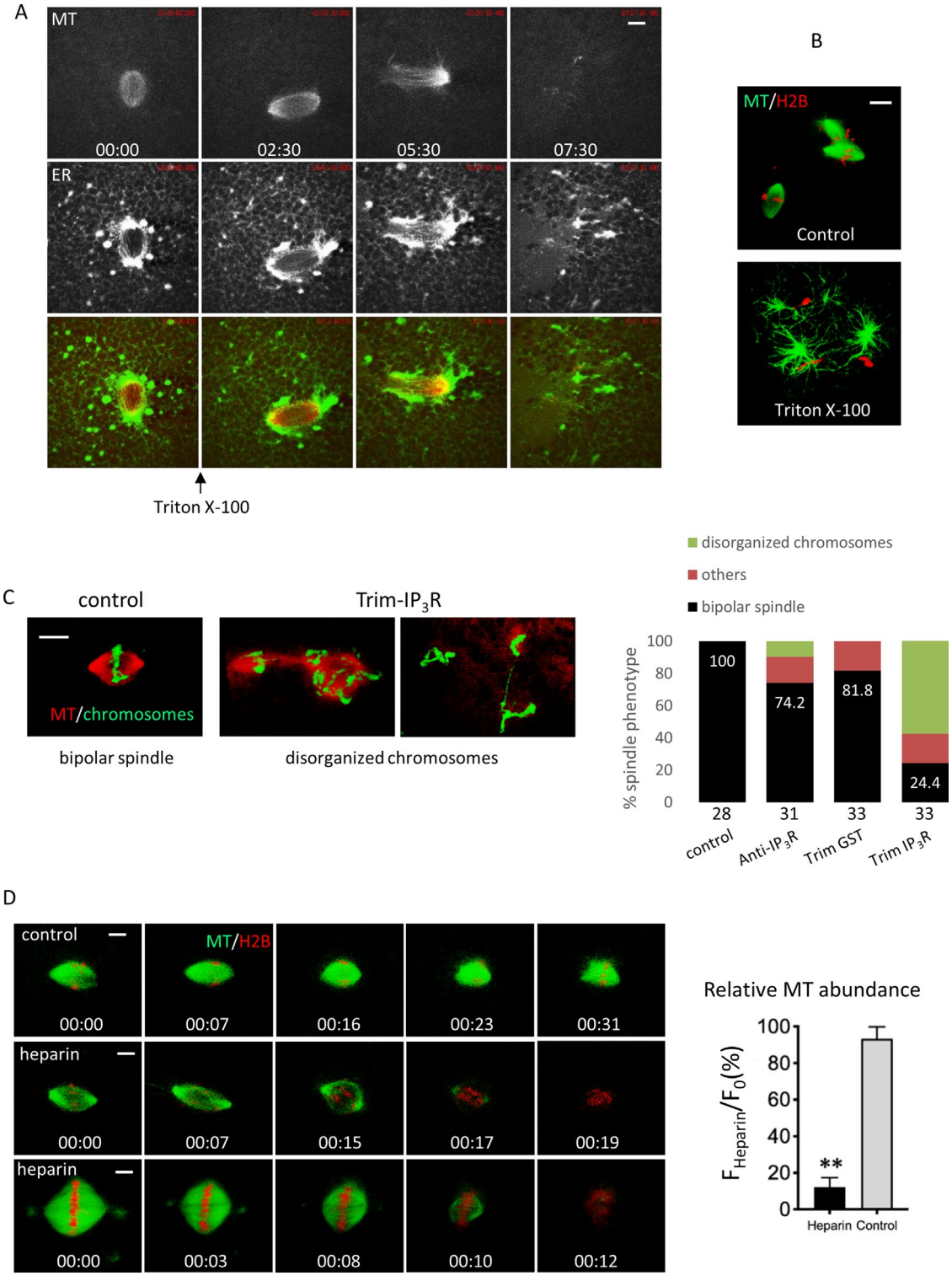

FIGURE 4: Bipolar spindle formation in extracts required ER membranes and IP_3R. (A) Simultaneous disruption of reticular ER structure and bipolar spindles: Triton X-100 was added to a cytoplasmic droplet containing bipolar spindles (00:00) at a final concentration of 0.1%. Confocal time-lapse imaging (3D projections of the entire confocal stacks) was carried out following the behavior of the same spindle ($n = 5$). Scale bar = 20 μm. Shown is a representative series obtained in four independent experiments. (B) Cell-free cytoplasmic extract spindle assembly in the absence (control) or presence of 0.1% Triton X-100. Scale bar = 20 μm. Shown are representations of 6 independent experiments. (C) Oocytes injected with mRNAs coding for RFP-tubulin and eGFP-H2B were further injected with Trim21 mRNA as indicated (Trim). At 24 h after Trim21 mRNA injection, oocytes were injected with anti-IP_3R antibodies or anti-GST antibodies as indicated. At 4 h after antibody injection, all oocytes were incubated with progesterone overnight. The oocytes were then subjected to cytoplasm aspiration and spindle assembly assays. The ability of each oocyte to assemble bipolar spindles was assessed by confocal imaging and classified as bipolar spindle, disorganized

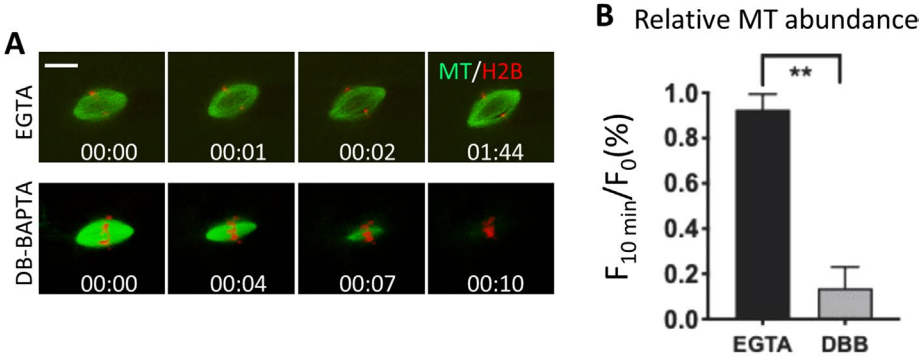

FIGURE 5: DB-BAPTA, but not EGTA, disrupt bipolar spindles in cell-free extracts. (A) Images of hh:mm. Scale bar = 20 µm. (B) The bar plot summarizes the relative microtubule abundance at 10 min after injection. Means ± SD; ** indicates $p < 0.01$; $n = 4$ (EGTA), $n = 8$ (DB-BAPTA).

droplets is not clear but is likely attributable, at least partly, to the varying distance between the site of heparin infusion and the spindle—hence the varying time required for heparin diffusion to reach the critical inhibition concentration.

Spindles assembled in oocyte extracts are sensitive to BAPTA but not EGTA

The forgoing results demonstrated the involvement of IP_3R in spindles assembled from oocyte extracts. If this involvement reflects the generation of a calcium nanodomain, it will be predicted that spindles assembled in oocyte extracts will be sensitive to BAPTA, but not EGTA, since nanodomains are sensitive to BAPTA but not EGTA (see *Introduction*). As predicted by the nanodomain model, spindles assembled in oocyte extracts were sensitive to BAPTA, so that spindle microtubules disassembled over the course of 5–10 min following BAPTA addition (Figure 5). In contrast, EGTA had no discernable effect on bipolar spindles assembled in extracts (Figure 5).

What is the contribution of the putative calcium nanodomain to meiosis? While the failure to emit polar bodies and the disorganization of meiotic spindles in oocytes lacking IP_3R permit more than one explanation, the results obtained from the single-oocyte extract experiments point directly to a deficit in spindle assembly as opposed to, say, problems in spindle positioning/anchoring. Further, they indicate that the nanodomains are not required for microtubule polymerization per se, but rather for stable, chromosome-proximal microtubule assembly and formation of a bipolar spindle. The close association of IP_3R-positive ER membranes with the spindles, especially the spindle poles, lends further support to this hypothesis. Based on the current findings, and the previous demonstration that meiotic spindles disassemble in response to BAPTA microinjection or uncaging, we specifically suggest that putative nanodomains create a microenvironment at the spindle poles that promotes pole-associated microtubule assembly and maintenance. Such a mechanism may be particularly important in situations—such as vertebrate meiosis—where centrosomes are lacking. What the relevant protein target of locally elevated calcium might be is unknown, although one possibility is CAMSAP (aka Nezha or Patronin), which binds to calmodulin in a calcium-dependent manner (King *et al.*, 2014) and which stabilizes the minus ends of noncentrosomal microtubules in various contexts (Tanaka *et al.*, 2012).

Previous studies of spindle assembly in bulk *Xenopus* egg extracts indicate that spindles self-organize, with microtubules first concentrating around chromosomes (or chromosome surrogates) and the spindle then assuming its characteristic stubby spindle shape as a result of dynein-dependent forces (Heald *et al.*, 1996). Our results suggest an additional element of spindle self-organization, namely, concentration of IP_3R-rich ER at the spindle poles. Indeed, given the fact that dynein inhibition can result in phenotypes (Heald *et al.*, 1996; Mitchison *et al.*, 2005) that resemble those seen in IP_3R-depleted single-oocyte extracts (here), it is tempting to speculate that besides organizing microtubules in extract-assembled spindles, dynein may also transport ER to spindle poles in such extracts. Interestingly, Wu et al have reported that obesity-induced ER stress causes spindle abnormality in mouse oocytes (Wu *et al.*, 2015). ER stress is known to disrupt multiple cellular pathways including calcium homeostasis and calcium signaling (Deniaud *et al.*, 2008). Therefore, the involvement of ER and IP_3R in spindle assembly is likely not restricted to *Xenopus* oocytes.

Finally, the novel cell-free spindle assembly system reported here may find widespread applications. The involvement of single oocytes, in contrast to the thousands required for "classical" egg extracts (Maresca and Heald, 2006), gives our method unprecedented versatility, permitting probe expression by DNA/mRNA injection and the use of oocytes at any developmental stage. Compared with protein expression via mRNA injection into the cytoplasm, protein expression via DNA injection into the nucleus is technically more challenging, with frequent oocyte damage and low protein expression levels/poor fluorescence image quality. This was especially true for GFP-IP_3R1, which is a large and complex membrane protein. Work is in progress to improve efficiency of protein expression via DNA injection. In addition, the coupling of TrimAway antibody-mediated rapid protein depletion (Clift *et al.*, 2018) with this cell-free system further enhances its use in determining protein functions in the many biological processes that can be studied in vitro.

MATERIALS AND METHODS

Unless otherwise stated, all chemicals were purchased from Sigma. Purified rabbit polyclonal antibodies against IP_3 receptor-1 (Runft *et al.*, 1999) were a gift of Laurinda Jaffe and Lisa Mehlmann (University of Connecticut Health Center). GFP-Trim21 and mCherry-Trim21 plasmids (pGEMHE-mEGFP-mTrim21 and pGEMHE-mCherry-mTrim21) were purchased from Addgene (#10551lim7 and #105522 respectively). sfGFP-ER-3 was a gift from Michael Davidson (Addgene plasmid #56482; http://n2t.net/addgene:56482;

chromosomes, or others (nuclei or microtubule asters). Shown are typical images of bipolar spindles and disorganized chromosomes, and a summary of four independent experiments with the total number of oocytes (*n*) in each group indicated. Scale bar = 20 µm. (D) Time-lapse (hh:mm) imaging of cell-free extract spindles following infusion of calcium-free OR2 (vehicle control) or heparin (200 µg/ml, two examples). Scale bar = 20 µm. The bar graph summarizes spindle microtubule abundance 7.5–20 min after heparin infusion relative to that before heparin infusion. For control, microtubule abundance 20 min after calcium-free OR2 infusion was compared with that before calcium-free OR2 infusion. Means ± SD; ** indicates $p < 0.01$; $n = 10$.

RRID:Addgene_56482). Other plasmids, GFP-IP_3R1, RFP-tubulin and 3XeGFP-EMTB (microtubule probes), eGFP-H2B and mRFP-H2B (chromosome probes) have been described in our previous publications (Bannai *et al.*, 2004; Li *et al.*, 2016; Shao *et al.*, 2013). To generate mRNA for oocyte injection, the plasmids were linearized with *Not*I and transcribed in vitro using T7 or SP6 polymerase (Ambion kit). We used the MaxChelator program (https://web.stanford.edu/~cpatton/maxc.html) to calculate the ratio of Ca^{2+} buffers over $CaCl_2$ (EGTA:$CaCl_2$ = 4:1; dibromo-BAPTA:$CaCl_2$ = 10:1) to give the desired free Ca^{2+} concentration, ~140 nM (Busa and Nuccitelli, 1985), in the calcium buffers used in extract spindle experiments.

Oocyte isolation and injection

Oocytes were manually defolliculated (Liu and Liu, 2006) and were kept at 18°C in OCM medium (60% of L-15 medium, supplemented with 1.07 g BSA per liter, mixed with 40% autoclaved water to yield the appropriate isotonic solution for amphibian oocytes). Manually defolliculated oocytes were used for all live cell imaging and cytoplasmic droplet experiments. Manually defolliculated oocytes were injected with mRNA encoding various probes, as described in our previous publications (Leblanc *et al.*, 2011; Shao *et al.*, 2012; Zhang *et al.*, 2008). For sfGFP-ER-3 and GFP-IP_3R1 plasmids, which lack viral (such as SP6 and T7) promoters for in vitro transcription, purified plasmids were injected into the oocyte germinal vesicle (~3 nL of 1 mg/ml DNA per oocyte). The injected oocytes were incubated in OCM for at least 6 h, or up to 2 d to allow protein expression before the addition of progesterone (1 μM) to induce oocyte maturation.

Live imaging and image presentation

Oocytes were monitored every 10 min for GVBD, indicated by the appearance of a white maturation spot. GVBD oocytes were transferred to fresh OCM without progesterone and further incubated, until the time of fluorescence imaging or cytoplasm aspiration for in vitro spindle assembly (see later).

Oocytes were imaged in poly-lysine-coated glass bottom microwell dishes (MatTek Corporation, P35G-1.5-10-C) with a 60x oil objective on a Zeiss Axiovert with a BioRad 1024 laser scanning confocal imaging system (Leblanc *et al.*, 2011), or a Quorum Spinning Disk confocal system. High-resolution images (Figure 3D, AiryScan) were obtained using a Zeiss LSM880 AxioObserver Z1 with AiryScan FAST. Time-lapse image series were collected at various time intervals. Each time point volume comprised 15–30 image planes 1–2 μm apart. Images were 3D-rendered or presented as single confocal planes, as indicated in legends, using Volocity (version 6.3). All time series were made from images acquired from the same oocyte, unless otherwise indicated.

TrimAway assays

We essentially followed the published protocol (Clift *et al.*, 2017, 2018). Briefly, oocytes were injected with Trim21 mRNA followed by incubation at room temperature for at least overnight. The oocytes were further injected with antibodies (anti-IP_3R or antibodies against bacterial glutathione S-transferase or anti-GST, 1 mg/ml, 20 nl per oocyte; Bayaa *et al.*, 2000) as indicated. Following further incubation for the indicated time, the oocytes were lysed for immunoblots. Oocytes destined for spindle assembly assays in vivo or in vitro were simultaneously injected with Trim21 mRNA together with mRNAs for RFP-tubulin (labeling microtubules) and eGFP-H2B (marking chromosomes). These oocytes were incubated at room temperature at least overnight, followed by injection with antibodies as indicated. The oocytes were further incubated for 4–6 h to allow antibody-mediated IP_3R degradation before the addition of progesterone to initiate oocyte maturation. Oocytes were examined, typically 6–12 h later, by confocal microscopy to determine the presence of a (first) polar body and spindle morphology or used for cell-free spindle assays. Although these oocytes expressed two GFP fusion proteins, GFP-Trim21 exhibited diffused cytoplasmic signal whereas eGFP-H2B specifically labeled chromosomes. Therefore, the presence of GFP-Trim21 fluorescence did not interfere with determination of spindle phenotypes.

Single cell–extract spindle assays

Preparation of demembranated sperm took place as follows (Lohka and Masui, 1983; Murray, 1991):

Xenopus laevis males were injected (i.p.) with 25 units pregnant mare serum gonadotropin (PMSG) followed by injection (i.p.) of 125 units of human chorionic gonadotrophin (hCG) 2 days later. One day after hCG injection, the animals were killed. Testes were excised and washed three times in ice-cold MMR (100 mM NaCl, 2 mM KCl, 1 mM $MgCl_2$, 2 mM $CaCl_2$, 0.5 mM HEPES, pH 7.8, 0.1 mM EDTA) followed by two washes in ice-cold NPB (250 mM sucrose, 0.2 mM spermine tetrahydrochloride, 0.5 mM spermidine trihydrochloride, 15 mM HEPES, pH 8.0, 1 mM EDTA, 1 mM dithiothreitol). After NPB was removed, testes were minced with a pair of dissecting scissors. The testes fragments were resuspended in NPB (2 ml) by gentle pipetting. The suspension was filtered through a 40-μm cell strainer and rinsed with 8 ml of NPB. The combined suspension was centrifuged for 10 min at 3000 rpm at 4°C. The sperm pellet was resuspended with 1 ml NPB and warmed to room temperature. Lysolicithin (50 μl of 10 mg/ml) was added and the mixture was incubated at room temperature for 5 min. Demembranated sperm appear as small fat "squiggles" that stain bright blue with Hoechst 33324 (1 μl 20 μg/ml dye mixed with 1 μl of sperm preparation); nondemembranated sperm will not stain with Hoechst 33324. Demembranated sperm was centrifuged at 3000 rpm for 5 min at 4°C and resuspended in 1 ml of NPB containing 3% BSA. Centrifugation was repeated twice more, and sperm pellets resuspended, first in 1 ml of NPB containing 0.3% BSA and then in 1 ml of 30% glycerol/NPB. Sperm was counted using a hemocytometer and stored (in single-use aliquots) in 30% glycerol/NPB at –80°C.

The following operations were performed in the glass bottom microwell imaging dishes and covered with mineral oil. Demembranated sperm nuclei, diluted in NPB to ~1000 nuclei/μl, were placed at the glass bottom of the dish in droplets of ~10 nl. In some experiments, Hoechst 33324 was added to sperm to a final concentration of 1 μg per ml before application to the glass. Oocytes, typically 1 h after GVBD (metaphase I or MI) or fully mature, metaphase II arrested, were placed under mineral oil in the same dishes with their animal poles facing up. While MI oocytes were transferred directly from OCM to the optical dish, metaphase II (or MII) oocytes were first rinsed in calcium-free oocyte medium (OR2: 83 mM NaCl, 2.5 mM KCl, 1 mM $MgCl_2$, 1 mM Na_2HPO_4, 5 mM HEPES, pH 7.8; Bayaa *et al.*, 2000) plus 5 mM EGTA before being placed in the optical dish. This is to prevent accidental oocyte/extract activation (calcium-induced destruction of cytostatic factor; Maresca and Heald, 2006), and hence facilitated spindle assembly. A glass pipette attached to the microinjector and with a tip opening of ~30 μm was then forced into the oocyte from the animal hemisphere. Negative pressure ("fill" function) was applied to slowly aspirate oocyte cytoplasm into the glass pipette (up to 300 nl) followed by expelling the cytoplasm onto the sperm droplets using the "inject" function. Multiple cytoplasmic droplets, 50–100 nl, could be produced from one oocyte. The dish was then placed on

the microscope for confocal imaging. When chemical inhibitors were used, they were delivered, via an on-stage microinjector, on top of the cytoplasmic droplet, furthest away from the spindle being imaged (which was at the bottom in our inverse microscope system). The inhibitors were delivered in volume less than 1/10 that of the cytoplasmic droplet.

See Supplemental Figure S2 for details.

Statistics

Data were analyzed by chi-squared or Student's *t* test (two-tailed) using GraphPad Prism 6, with $p < 0.05$ considered significant.

ACKNOWLEDGMENTS

We thank Laurinda Jaffe and Lisa Mehlmann (University of Connecticut Health Center) for purified anti-IP_3R antibodies. We thank Chloë van Oostende-Triplet and Skye McBride of University of Ottawa Image Core for advice and assistance during this study. This work was supported by a project grant from the Canadian Institute of Health Research (PJT-168891) to X.J.L. and an NIH grant (GM52932) to W.M.B. Y.R. received a visiting scholarship from the China Scholarship Council (2020–2021). G.M. received a PhD scholarship from the China Scholarship Council (2014–2018) and a Designation 2020 Faculty of Medicine Scholarship from the University of Ottawa (2014).

REFERENCES

Adler EM, Augustine GJ, Duffy SN, Charlton MP (1991). Alien intracellular calcium chelators attenuate neurotransmitter release at the squid giant synapse. J Neurosci 11, 1496–1507.

Bannai H, Inoue T, Nakayama T, Hattori M, Mikoshiba K (2004). Kinesin dependent, rapid, bi-directional transport of ER sub-compartment in dendrites of hippocampal neurons. J Cell Sci 117, 163–175.

Bayaa M, Booth RA, Sheng Y, Liu XJ (2000). The classical progesterone receptor mediates *Xenopus* oocyte maturation through a nongenomic mechanism. Proc Natl Acad Sci USA 97, 12607–12612.

Busa WB, Nuccitelli R (1985). An elevated free cytosolic Ca2+ wave follows fertilization in eggs of the frog, *Xenopuslaevis*. J Cell Biol 100, 1325–1329.

Clift D, McEwan WA, Labzin LI, Konieczny V, Mogessie B, James LC, Schuh M (2017). A method for the acute and rapid degradation of endogenous proteins. Cell 171, 1692–1706.

Clift D, So C, McEwan WA, James LC, Schuh M (2018). Acute and rapid degradation of endogenous proteins by Trim-Away. Nat Protoc 13, 2149–2175.

Deniaud A, Sharaf el dein O, Maillier E, Poncet D, Kroemer G, Lemaire C, Brenner C (2008). Endoplasmic reticulum stress induces calcium-dependent permeability transition, mitochondrial outer membrane permeabilization and apoptosis. Oncogene 27, 285–299.

Desai A, Maddox PS, Mitchison TJ, Salmon ED (1998). Anaphase A chromosome movement and poleward spindle microtubule flux occur At similar rates in *Xenopus* extract spindles. J Cell Biol 141, 703–713.

FitzHarris G, Marangos P, Carroll J (2007). Changes in endoplasmic reticulum structure during mouse oocyte maturation are controlled by the cytoskeleton and cytoplasmic dynein. Dev Biol 305, 133–144.

Groen AC, Coughlin M, Mitchison TJ (2011). Microtubule assembly in meiotic extract requires glycogen. Mol Biol Cell 22, 3139–3151.

Groigno L, Whitaker M (1998). An anaphase calcium signal controls chromosome disjunction in early sea urchin embryos. Cell 92, 193–204.

Heald R, Tournebize R, Blank T, Sandaltzopoulos R, Becker P, Hyman A, Karsenti E (1996). Self-organization of microtubules into bipolar spindles around artificial chromosomes in *Xenopus* egg extracts. Nature 382, 420–425.

King MD, Phillips GW, Bignone PA, Hayes NV, Pinder JC, Baines AJ (2014). A conserved sequence in calmodulin regulated spectrin-associated protein 1 links its interaction with spectrin and calmodulin to neurite outgrowth. J Neurochem 128, 391–402.

Kume S, Muto A, Aruga J, Nakagawa T, Michikawa T, Furuichi T, Nakade S, Okano H, Mikoshiba K (1993). The *Xenopus* IP3 receptor: structure, function, and localization in oocytes and eggs. Cell 73, 555–570.

Leblanc J, Zhang X, McKee D, Wang ZB, Li R, Ma C, Sun QY, Liu XJ (2011). The small GTPase Cdc42 promotes membrane protrusion during polar body emission via ARP2-nucleated actin polymerization. Mol Hum Reprod 17, 305–316.

Li R, Leblanc J, He K, Liu XJ (2016). Spindle function in *Xenopus* oocytes involves possible nanodomain calcium signaling. Mol Biol Cell 27, 3273–3283.

Liu XJ (2012). Polar body emission. Cytoskeleton (Hoboken) 69, 670–685.

Liu XS, Liu XJ (2006). Oocyte isolation and enucleation. Methods Mol Biol 322, 31–41.

Lohka MJ, Masui Y (1983). Formation in vitro of sperm pronuclei and mitotic chromosomes induced by amphibian ooplasmic components. Science 220, 719–721.

Lu L, Ladinsky MS, Kirchhausen T (2009). Cisternal organization of the endoplasmic reticulum during mitosis. Mol Biol Cell 20, 3471–3480.

Mann JS, Lowther KM, Mehlmann LM (2010). Reorganization of the endoplasmic reticulum and development of Ca2+ release mechanisms during meiotic maturation of human oocytes. Biol Reprod 83, 578–583.

Maresca TJ, Heald R (2006). Methods for studying spindle assembly and chromosome condensation in *Xenopus* egg extracts. Methods Mol Biol 322, 459–474.

Mitchison TJ, Maddox P, Gaetz J, Groen A, Shirasu M, Desai A, Salmon ED, Kapoor TM (2005). Roles of polymerization dynamics, opposed motors, and a tensile element in governing the length of *Xenopus* extract meiotic spindles. Mol Biol Cell 16, 3064–3076.

Murray AW (1991). Cell cycle extracts. Methods Cell Biol 36, 581–605.

Parry H, McDougall A, Whitaker M (2006). Endoplasmic reticulum generates calcium signalling microdomains around the nucleus and spindle in syncytial *Drosophila* embryos. Biochem Soc Trans 34, 385–388.

Plachot M, de GJ, Junca AM, Mandelbaum J, Turleau C, Couillin P, Cohen J, Salat-Baroux J (1987). From oocyte to embryo: a model, deduced from in vitro fertilization, for natural selection against chromosome abnormalities. Ann Genet 30, 22–32.

Runft LL, Watras J, Jaffe LA (1999). Calcium release at fertilization of *Xenopus* eggs requires type I IP(3) receptors, but not SH2 domain-mediated activation of PLCgamma or G(q)-mediated activation of PLCbeta. Dev Biol 214, 399–411.

Shao H, Li R, Ma C, Chen E, Liu XJ (2013). *Xenopus* oocyte meiosis lacks spindle assembly checkpoint control. J Cell Biol 201, 191–200.

Shao H, Ma C, Zhang X, Li R, Miller AL, Bement WM, Liu XJ (2012). Aurora B regulates spindle bipolarity in meiosis in vertebrate oocytes. Cell Cycle 11, 2672–2680.

Tanaka N, Meng W, Nagae S, Takeichi M (2012). Nezha/CAMSAP3 and CAMSAP2 cooperate in epithelial-specific organization of noncentrosomal microtubules. Proc Natl Acad Sci USA 109, 20029–20034.

Taylor CW, Tovey SC (2010). IP(3) receptors: toward understanding their activation. Cold Spring Harb Perspect Biol 2, a004010.

Terasaki M, Runft LL, Hand AR (2001). Changes in organization of the endoplasmic reticulum during *Xenopus* oocyte maturation and activation. Mol Biol Cell 12, 1103–1116.

Wang LY, Augustine GJ (2014). Presynaptic nanodomains: a tale of two synapses. Front Cell Neurosci 8, 455.

Weir E, McLinden G, Alfandari D, Cousin H (2021). Trim-Away mediated knock down uncovers a new function for Lbh during gastrulation of *Xenopuslaevis*. Dev Biol 470, 74–83.

Wu LL, Russell DL, Wong SL, Chen M, Tsai TS, St John JC, Norman RJ, Febbraio MA, Carroll J, Robker RL (2015). Mitochondrial dysfunction in oocytes of obese mothers: transmission to offspring and reversal by pharmacological endoplasmic reticulum stress inhibitors. Development 142, 681–691.

Zhang X, Ma C, Miller AL, Katbi HA, Bement WM, Liu XJ (2008). Polar body emission requires a RhoA contractile ring and Cdc42-mediated membrane protrusion. Dev Cell 15, 386–400.